Journal of Nuclear Materials 390–391 (2009) 335–338

Contents lists available at ScienceDirect

Journal of Nuclear Materials

journal homepage: www.elsevier.com/locate/jnucmat

Kinetic simulations of the parallel transport in the JET scrape-off layer

D. Tskhakaya [b,1,*], R.A. Pitts [c], W. Fundamenski [d], T. Eich [e], S. Kuhn [b], JET EFDA Contributors [a,2]

[a] JET-EFDA, Culham Science Centre, OX14 3DB, Abingdon, UK
[b] Association EURATOM-ÖAW, A-6020 Innsbruck, Austria
[c] CRPP-EPFL, Association EURATOM – Conféderation Suisse, 1015 Lausanne, Switzerland
[d] EURATOM-UKAEA Fusion Association, Abingdon, Oxon OX14 3DB, UK
[e] IPP-EURATOM Association, D-85748 Garching, Germany

ARTICLE INFO

PACS:
52.40.Kh
52.40.Hf
52.25.Xz
52.65.Rr

ABSTRACT

In this paper, we present kinetic simulation results of plasma parallel transport in the stationary and ELMy scrape-off (SOL) layer. We demonstrate that number of kinetic factors describing SOL are strongly nonuniform and evolve during the ELM. Power loads to the divertor obtained from the ELMy SOL simulations are in a perfect agreement with the experimental measurements at JET.

1. Introduction

Usually it is assumed that the parallel transport is the most simple and well studied type of plasma transport. In the scrape-off layer (SOL) this is not the case: low collisionality of plasma, different inelastic and short time scale processes, and geometrical effects can cause deviation of parallel transport from the classical one. As a result, the classical transport model can significantly over (under) estimate particle and energy fluxes to the divertor targets [1]. For our day tokamaks these uncertainties are not essential, but for the ITER, where transient heat loads on divertor targets represent one of the greatest threats to target lifetime, they can lead to serious unwanted consequences. Hence, development of realistic kinetic models of the parallel transport in the SOL is of top importance. In this work we describe one of such models, which is applied to the JET SOL.

In the present study we update our model developed in [1] by including plasma recycling and electron radiation and consider different types of the ELM 'reconnection'. We show that number of kinetic factors are only weakly dependent on chosen model and can probably be used for prediction of parallel transport for next generation tokamaks.

2. Kinetic factors in the stationary SOL

There are two groups of kinetic factors specifying parallel transport in the stationary SOL [1,2]: boundary conditions (BCs) in front of the divertor targets and heat flux and ion viscosity limiters. It is convenient to consider these factors separately.

The BCs targets used in SOL analysis are based on a classical sheath model and represent conditions for ion parallel speed ($V_{||}$), energy fluxes at the sheath (Q_{sh}) and potential drop across the sheath ($\Delta\phi$):

$$V_{||} = c_s = \sqrt{\frac{T_e + \chi T_i}{M_i}}, Q^s_{sh} = \gamma_s \Gamma_s T_s, \quad \Delta\phi = \frac{T_e}{e}\varphi,$$
$$\varphi \approx 2 \div 5, \quad s = e, i, \tag{1}$$

where χ is the polytropic constant and $\gamma_e = 2 + \varphi$, $\gamma_i = 2.5 + 0.5(T_e/T_i + \chi)$ are the sheath (heat) transmission coefficients.

In the work [1], we have considered a simplified SOL model (without taking into the account number of inelastic processes) and indicated that all the BCs are in a perfect agreement with the classical ones for wide range of SOL collisionality (see Fig. 1). But as it is demonstrated below, the inelastic processes can significantly affect some of the BCs.

For the present simulations we use the electrostatic 1.5d3v (1D and 2D in space for plasma and neutrals, respectively, and 3D in velocity space) particle-in cell (PIC) code BIT1 including nonlinear collisions for arbitrary number of charged and neutral particle species and a linear model of plasma-surface interaction processes [3,4]. The simulation geometry corresponds to a single magnetic flux tube bounded between inner and outer divertor plates. Near midplane there is an ambipolar plasma source (S) mimicking cross

* Corresponding author. Address: Technikerstrasse 25/II, A-6020 Innsbruck, Austria.
E-mail address: david.tskhakaya@uibk.ac.at (D. Tskhakaya).

[1] Permanent address: Andronikashvili Institute of Physics, 0177 Tbilisi, Georgia.

[2] See the Appendix of M.L. Watkins et al., Fusion Energy 2006 (Proc. 21st Int. Conf. Chengdu, 2006) IAEA, (2006).

0022-3115/$ - see front matter © 2009 Elsevier B.V. All rights reserved.
doi:10.1016/j.jnucmat.2009.01.150

field transport across the separatrix. Further details of the PIC simulation of the SOL can be found in [1].

In order to approach realistic conditions of the JET SOL in the present study we have included plasma recycling from the divertor targets and electron-impurity interaction. Recycling is done by emission of atomic deuterium with $T_D = 2$ eV temperature due to impact of ions at the divertors. This simplified model saves a lot of CPU time and gives the similar results as a full recycling model for the attached plasma [4]. Recycling coefficient is $R = 0.99$. The neutrals are treated in 2D and are removed from the simulation when reaching the radial boundary mimicking neutral loss at the outer wall and in the private flux region. Electron radiative cooling is implemented via electron excitation collisions with C^+ impurity, representing background with the fixed nonuniform density profile and constant temperature $T_C = 10$ eV.

We have made two separate runs, one with only electron radiation and another with full model including plasma recycling too. This allows us to study the influence of these processes separately. As it was expected, these processes strongly modify plasma density and temperature profiles near the divertors affecting BCs there (see Fig. 1). As one can see, the radiation reduces φ by 40% and slightly ($\sim$10%) increases γ_e. This fact has the following explanation: the superthermal electrons currying the main part of energy, suffer less excitation collisions, than the thermal electrons (see Fig. 2). As a result, the electron temperature and the normalized potential drop (defined mainly by thermal electrons) reduce, but the ratio of energy flux to the particle flux and temperature (i.e. γ_e) increases. Due to recycling the plasma collisionality increases near the divertor, so that electron distribution relaxes to the Maxwellian. As a result, γ_e relaxes to the classical value too. Modified potential profile in the presheath influences ion energy flux, so that γ_i increases for the case with radiation. Contrary to this the recycling reduces γ_i by $\sim$10%, because the ion energy flux reduces due to charge-exchange with low temperature atoms.

The heat flux and viscosity limiters are introduced in order to limit particle heat flux and ion viscosity, which can be overestimated by corresponding classical expressions [5]:

$$q_{\|} = \left(\frac{1}{q_{SH}} + \frac{1}{anV_T T}\right)^{-1}, \quad \pi_{\|} = \left(\frac{1}{\pi_{\|}^{Br}} + \frac{1}{bnT}\right)^{-1}, \tag{2}$$

where $V_T = \sqrt{T/M}$, a and b are the limiters, and q_{SH} and $\pi_{\|}^{Br}$ are the Spitzer–Harm heat flux and Braginskii viscosity. The heat flux limiters are introduced for the electrons as well as for the ions; while the viscosity limiter is introduced only for the ions (usually the electron viscosity is too small to be taken into the account). Typically, the following values $a_{e,i} \approx 0.1$, $b(\equiv b_i) \approx 0.5$ are used in fluid simulations of the SOL, assuming that $a_{e,i}, b \to \infty$ with increasing collisionality. Our previous simulations indicate that these coefficients are strongly nonuniform in space (they change by order of magnitude along the SOL), so that it is reasonable to introduce corresponding poloidaly averaged values [1]. Unfortunately, this is still not a solution, because these averaged limiters do not show expected behaviour, namely they decrease (not increase!) with increasing collisionality, although $a_{e,i} \approx 0.1$, $b \approx 0.5$ are good approximations for poloidaly averaged limiters for JET SOL (see Fig. 3). Moreover, a strongly evolve in the ELMy SOL, so that the fluid codes can get convergence problems, when using time-dependant limiters [1]. In addition, as one can see from Fig. 3, limiters are strongly affected by inelastic processes, so that validity of the limited expressions (2) becomes questionable. Thus, below we omit the study of behaviour of limiters in the ELMy SOL.

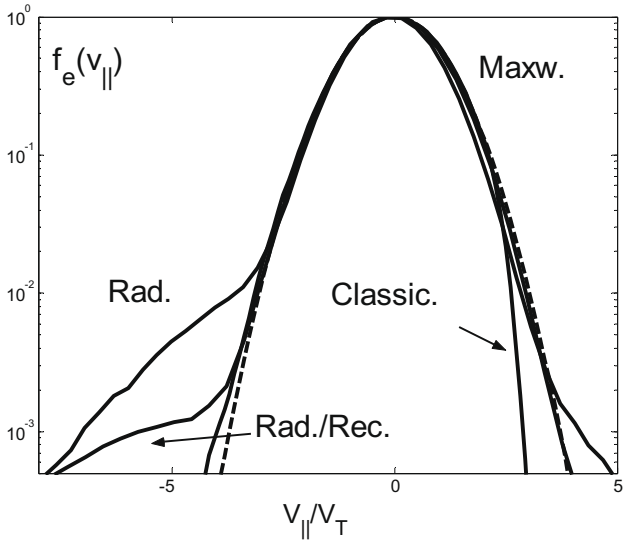

Fig. 2. Normalized electron velocity distribution functions at the divertor sheath.

3. Parallel transport in the ELMy SOL

Contrary to the stationary SOL the parallel transport study in the ELMy SOL has a short history. Based on a simple model an analytic function for power load to the divertor targets and γ has been derived in [6], in [7] the expression for power loads has been updated in order to fit experimental observations, a similar fit function for power loads has been derived from PIC simulation [8]. First attempts to classify the behaviour of BCs and heat flux and

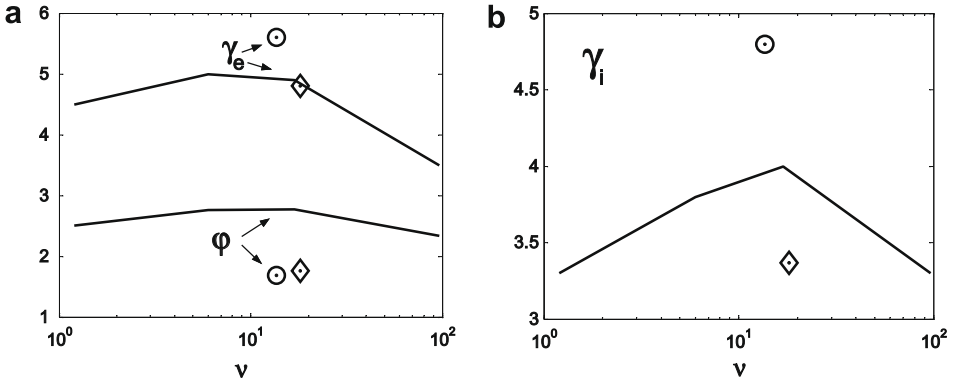

Fig. 1. Boundary conditions at the divertor targets versus SOL collisionality. Solid line: model without inelastic processes [1]; circles: model with electron radiation, and diamonds: full model with plasma recycling and electron radiation.

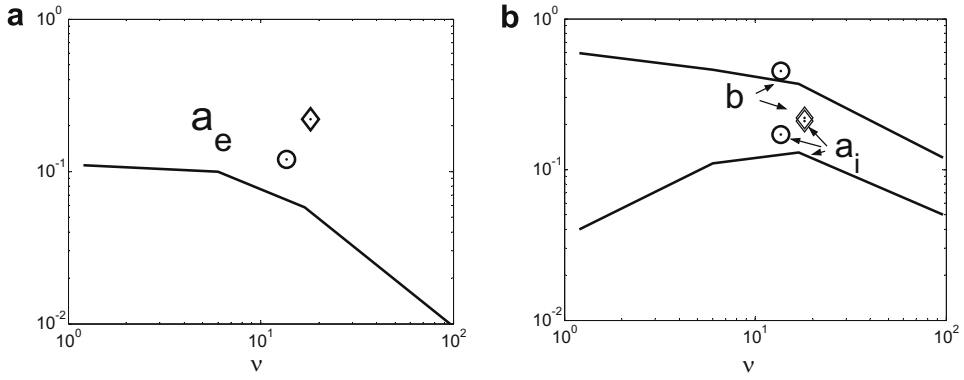

Fig. 3. Flux and ion viscosity limiters averaged poloidaly versus SOL collisionality. Notations are same as in Fig. 1.

ion viscosity limiters have been made in [1]. It was shown that almost all kinetic factors evolve strongly during the ELM and even the definition of the plasma boundary becomes not trivial. In [1] fit functions have been introduced describing behaviour of BCs for JET relevant parameters.

As it was mentioned above, the PIC model from [1] (and [8]) does not include inelastic processes. Moreover, a stepwise source function has been used for ELM onset. In reality, the time shape of the ELM source is unknown; hence it is reasonable to study the influence of this source shape, together with radiation and recycling effects. We considered two different types of the source, exponential and Gaussian ones: $S(t) = S_{ELM}\exp(-\alpha t)$, $S(t) = S_{ELM}\exp(-\beta(t-\tau_{ELM}/2)^2)$, with different α and β. Here, $t = 0$ corresponds to the start of the ELM and τ_{ELM} is the reconnection time. For simulations we consider $W_{ELM} \approx 0.4$ MJ ELM, which corresponds to the shot 62221 at JET with well diagnosed power loads to the divertor targets. In Fig. 4 are plotted histories of power load to the outer divertor target and γ_i. As one can see, the time scale and the amplitude of power deposition depend on shape of the ELM source. The inelastic processes affect mainly the amplitude, but not the time scale. Contrary to this, the amplitude of γ_i depends weakly on the shape of ELM source, but very sensitive to the plasma recycling. The BCs connected with the electron time scales (i.e. γ_e and φ) depend strongly on the source shape and inelastic processes too. Important to note, that there are two transport characteristics, which are practically insensitive to the chosen model. Namely, (i) the major part of the energy is deposited to the divertors by the ions, and (ii) the integral energy curried to the target up to the time, τ_{IR}, at which the energy peaks (which defines the maximum surface temperature rise that the target will experience, $\Delta W(t \leqslant \tau_{IR}) = \int_0^{\tau_{IR}} q_{div} dt$) satisfies $0.15W_{ELM} < \Delta W(t \leqslant \tau_{IR}) < 0.35W_{ELM}$.

Time history of the ELM reconnection (i.e. temporal shape of the ELM source) cannot be directly measured in the experiment, but can be estimated from observed power loads to the targets. For this purpose we have averaged the simulated power loads over ~50 μs (typical resolution for divertor power load diagnostic at JET) and compare with the experimental results (see Fig. 5). I order to take

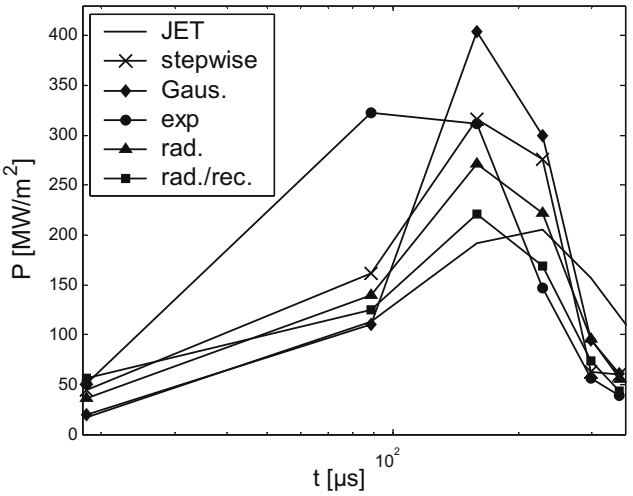

Fig. 5. ELM power loads to the outer divertor from the simulation (averaged over ~50 μs) and from the experiment (shot 62221 at JET).

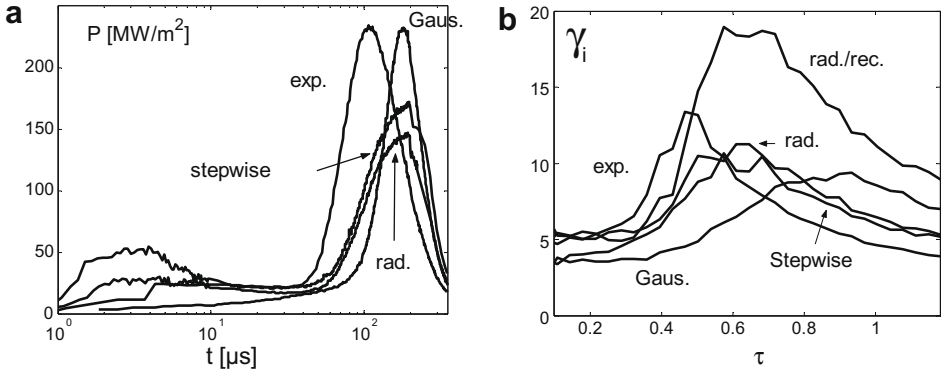

Fig. 4. Time history of the power loads to the outer divertor target (a) and γ_i (b) during the 0.4 MJ ELM obtained from different models. $\tau = c_s t/L_{||}$, where $L_{||}$ is the connection length.

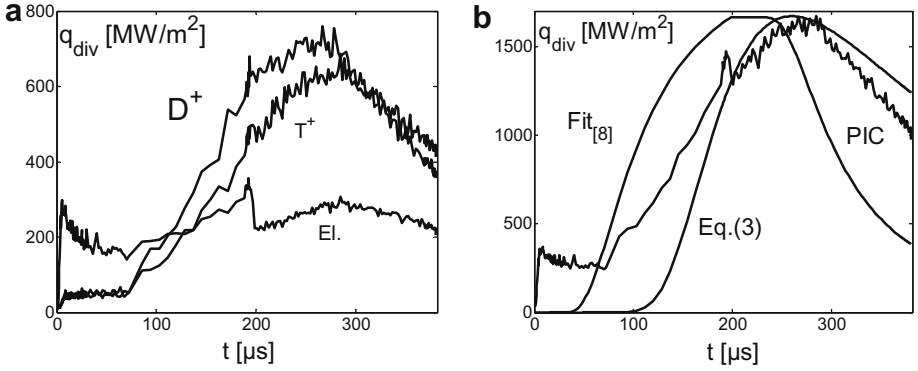

Fig. 6. ELM power loads to the ITER outer divertor: (a) electron, D and T power loads, and (b) total power load from PIC, Eq. (3) and fit from [8].

into account the radially nonuniform profile of power loads, we assume that it has an exponential shape, $q_{div}(r) = q_{div}(0)\exp(-r/\lambda)$ and after averaging over $r = [0, \lambda]$ we obtain $\langle q_{div}(r)\rangle \approx 0.632 q_{div}(0)$. As a result, the power loads from 1D simulation (corresponding to $q_{div}(0)$) are multiplied by the factor 0.632 before they are compared to the experimental measurements representing the radially averaged values. As we can see, the best agreement is achieved for the stepwise ELM source and this agreement becomes better with increasing realism of the model, indicating that the 'simple' 1D model of the ELM transport probably works. This provides an important degree of confidence in the extrapolations to ELMs in ITER, which is described below.

For modelling of ITER ELMy SOL we first simulate the pre-ELM SOL (with typical $n_{midplane} \approx 3\times 10^{19}$ m^{-3}, $T_{midplane} \approx 250$ eV) and then 'switched' stepwise the ELM by increasing the strength of the particle source and incoming particle temperature for $\tau_{ELM} = 200$ μs. We simulate a large ELM with $W_{ELM} \approx 4$ MJ (see [9]) and assume the following pedestal parameters: $n_{ped} \approx 6\times 10^{19}$ m^{-3}, $T_{ped} \approx 5$ keV. In order to save the CPU time no inelastic processes are included in the model. In Fig. 6 are plotted power loads to the outer divertor obtained from the simulation. It is noticeable that although D and T power loads are not fully ambipolar (they are peaking at corresponding transit times), but the total power load corresponds to the energy propagation with the sound speed $c_s = \sqrt{2T_{ped}/(s_D M_D + s_T M_T)}$, and can be fitted by analytic expression derived in [6,7]:

$$P_{div}(t) = \frac{P_{\max}}{0.84}\left(\frac{\tau}{t}\right)^2\left(1+\left(\frac{\tau}{t}\right)^2\right)\exp\left(-\left(\frac{\tau}{t}\right)^2\right), \quad \tau = \tau_{ELM} + \frac{L_{||}}{\sqrt{2}c_s}, \tag{3}$$

Here, $s_{D,T}$ (=0.5) is the concentration of D and T (note, in [7] there is no $\sqrt{2}$ in front of c_s). Contrary to this, the fit function from [8] overestimates the speed of energy propagation. The reason of this discrepancy is the parameter $L_{||}/c_s\tau_{rec}$ describing ELM parallel transport: it is smaller for ITER than for large ELMs at JET studied in [8].

4. Conclusions

Our simulations indicate that almost all BCs in the stationary SOL depend weakly on inelastic processes going in the divertor plasma and are almost independent of SOL collisionality. The exception it the normalised potential drop across the sheath decreasing up to 40% (for JET relevant parameters) with electron radiation cooling. Contrary to this, the heat flux and ion viscosity limiters can change by order of magnitude along the field line and the corresponding poloidaly averaged values depend strongly on inelastic processes and SOL collisionality (they do not increase with the collisionslity as one can expect). Hence, for relatively high SOL collisionalities ($\nu > 1$) it is better to not to limit heat fluxes and viscosity at all, otherwise the mistake originated from the limited expressions (2) can be worse.

Our results indicate that for predictive modelling of the ELM transport in the SOL it is necessary to consider a complete model including plasma recycling and electron radiative cooling and use a proper (temporal) shape of the ELM source. The best agreement with the experiment we obtained for stepwise ELM source used in [1,8].

Power loads to the ITER divertor correspond to the energy propagation in the SOL with the supersonic speed and (at least for $W_{ELM} \approx 4$ MJ) can be described by expression (3).

Acknowledgements

This work, carried out under the European Fusion Development agreement, supported by the European Communities. The views and opinions expressed herein do not necessarily reflect those of the European Commission. The first author acknowledges support by the projects TW6-TPP-DAMTRAN and GNSF 69/07.

References

[1] D. Tskhakaya, F. Subba, X. Bonnin, D. Coster, W. Fundamenski, R.A. Pitts, JET EFDA Contributors, Contrib. Plasma Phys. 48 (1–3) (2008) 89.
[2] P.C. Stangeby, The Plasma Boundary of Magnetic Fusion Devices, Institute of Physics Publishing, Bristol and Philadelphia, 2000.
[3] D. Tskhakaya, R. Schneider, J. Comp. Phys. 225 (1) (2007) 829.
[4] D. Tskhakaya, S. Kuhn, Y. Tomita, K. Matyash, R. Schneider, F. Taccogna, Contrib. Plasma Phys. 48 (1–3) (2008) 121.
[5] W. Fundamenski, Plasma Phys. Control. Fus. 47 (2005) R163.
[6] W. Fundamenski1, R.A. Pitts, JET EFDA Contributors, Plasma Phys. Control. Fus. 48 (2006) 109.
[7] T. Eich, A. Kallenbach, A. Herrmann, J.C. Fuchs, C.S. Chang, D. Tskhakaya, ASDEX Upgrade Team, Eur. Conf. Abstr. 31F (2007) 2.017.
[8] D. Tskhakaya, R.A. Pitts, W. Fundamenski, T. Eich, S. Kuhn, JET EFDA Contributors, Eur. Conf. Abstr. 31F (2007) O2.002.
[9] A. Loarte et al., in: Presented at 22nd IAEA Fusion Energy Conference, Geneva, Switzerland, 2008.